The Astrophysical Journal, 578:972–978, 2002 October 20

EVIDENCE OF POSTERUPTION RECONNECTION ASSOCIATED WITH CORONAL MASS EJECTIONS IN THE SOLAR WIND

Pete Riley, J. A. Linker, and Z. Mikić
Science Applications International Corporation, San Diego, CA 92121; pete.riley@saic.com

D. Odstrcil and V. J. Pizzo
National Oceanic and Atmospheric Administration, Space Environment Center, Boulder, CO 80303

and

D. F. Webb
Institute for Scientific Research, Boston College, Chestnut Hill, MA 02467
Received 2002 April 29; accepted 2002 July 1

ABSTRACT

Using a coupled 2.5-dimensional, time-dependent MHD model of the solar corona and inner heliosphere, we have simulated the eruption and evolution of a coronal mass ejection containing a flux rope all the way from the Sun to 1 AU. Although idealized, we find that the simulation reproduces many generic features of magnetic clouds. In this paper we report on a new, intriguing aspect of these comparisons. Specifically, the results suggest that jetted outflow, driven by posteruptive reconnection underneath the flux rope, occurs and may remain intact out to 1 AU and beyond. We present an example of a magnetic cloud with precisely these signatures and show that the velocity perturbations are consistent with reconnection outflow. We suggest that other velocity and/or density enhancements observed trailing magnetic clouds may be signatures of such reconnection and, in some cases, may not be associated with prominence material, as has previously been suggested.

Subject headings: solar wind — Sun: activity — Sun: corona — Sun: coronal mass ejections (CMEs) — Sun: magnetic fields

On-line material: color figures

1. INTRODUCTION

Coronal mass ejections (CMEs) are spectacular events involving the expulsion of significant amounts of solar material (10^{15}–10^{16} g) into the heliosphere (Hundhausen 1988). Associated with this eruption is 10^{31}–10^{32} ergs of energy, which is presumably supplied by the magnetic field. However, the basic preeruption configuration and the topological changes in the magnetic field that results in the conversion of magnetic energy into kinetic energy are not well known. Undoubtedly, reconnection plays a central role in this, but the details of where it takes place, how fast, and for how long are, again, not well understood.

A number of theoretical models have been proposed to explain the eruption and evolution of CMEs near the Sun. Useful classifications based on (1) "storage and release" versus "directly driven" mechanisms (Klimchuk 2001) and (2) resistive versus ideal instabilities (Forbes 2000) have been proposed to organize them. To varying degrees, all these models are idealized and as such tend to focus on reproducing a particular aspect of the eruption process at the expense of others. In some cases, this leads to model predictions that contradict reliable observations. Given the inherent complexity of CMEs, it is hardly surprising that theoretical models of CME eruption tend to be idealized. Nevertheless, if we are to make progress in understanding such phenomena, it is important to make connections between the models and observations. This may serve to place additional constraints on the models and may even differentiate between competing models, providing support for a particular physical mechanism. Additionally, and the motivation for the present paper, the simulations may suggest new and previously unidentified processes and/or signatures to be discovered in the observations. One must, of course, be careful not to overinterpret the results of idealized models. In particular, it is important to emphasize that the absence (presence) of specific features in the observations, when (not) predicted by a particular model, does not necessarily invalidate that model.

CME-related reconnection signatures in solar wind measurements have been the topic of a number of studies. Primarily, they have focused on the magnetic field topology within interplanetary CMEs and how reconnection back at the Sun could affect whether these field lines would be observed to be open or closed (e.g., Gosling, Birn, & Hesse 1995). Collier et al. (2001), on the other hand, discussed a magnetic cloud observed by the *Wind* spacecraft containing an embedded shock, monochromatic wave, heat flux dropout, and energetic ion beam that they associated with reconnection near the footpoints of the cloud. Their key signature of reconnection was the presence of a fast forward shock within the CME, which might be expected based on Sonnerup's (1970) generalization of the Petschek (1964) model.

In this paper, we analyze the interplanetary properties of a magnetohydrodynamic (MHD) simulation mimicking the eruption, propagation, and evolution of a flux-rope CME. Our goal is to connect simulation results with in situ plasma and magnetic field measurements. In particular, we focus on a specific signature, namely, a velocity enhancement behind the ejecta. We demonstrate that its origin in the simulations lies in posteruptive reconnection outflow beneath the flux rope, and, by virtue of the many similarities between the simulation and the observations, we suggest that the same

mechanism is responsible there, too. Should this hypothesis be substantiated by further observations, this result may lead to important constraints on theories of CME eruption.

2. DESCRIPTION OF THE MODEL

We solve the basic set of time-dependent MHD equations that describe many aspects of the large-scale behavior of the solar corona and inner heliosphere. We separate the region of space into two parts. We distinguish between the "coronal" region, which spans the photosphere up to 20 $R_\odot$, and the "heliospheric" region, which spans 20 $R_\odot$ to 1 AU. The Science Applications International Corporation (SAIC) coronal MHD model (Mikić & Linker 1994) is used to solve for the coronal region, and the National Oceanic and Atmospheric Administration/Space Environment Center (NOAA/SEC) heliospheric MHD model (Odstrcil & Pizzo 1999a) is used to solve for the heliospheric region, being driven directly by output from the coronal solution. This approach has a number of practical and scientific advantages. In particular, each code has been designed specifically for its respective environment. Moreover, decoupling these regions in this way allows the heliospheric portion to run at significantly larger time steps than are required by the coronal algorithm. A detailed description of the coupling of the two models has been given by Odstrcil et al. (2002), and the results of the specific simulation discussed here have been used to interpret joint observations of a CME by the *Ulysses* and the *Advanced Composition Explorer* (*ACE*) spacecraft at significantly different locations in the heliosphere (Riley et al. 2002).

The details of the algorithm used to advance the equations of the SAIC coronal model are given elsewhere (Mikić & Linker 1994; Lionello et al. 1998; Mikić et al. 1999). Here, we make a few brief remarks. The equations are solved on a spherical (r, θ, ϕ) grid, which permits nonuniform spacing of mesh points in both r and θ, thus providing better resolution of narrow structures, such as current sheets. In the radial (r) and meridional (θ) directions we use a finite-difference approach. In azimuth (ϕ), the derivatives are calculated pseudospectrally. We impose staggered meshes in r and θ, which has the effect of preserving $\nabla \cdot \boldsymbol{B} = 0$ to within roundoff errors for the duration of the simulation.

The NOAA/SEC heliospheric model solves the time-dependent MHD equations in a spherical geometry using either the flux-corrected transport or total-variation-diminishing schemes (e.g., Odstrcil 1993, 1994; Toth & Odstrcil 1996). These high-resolution schemes produce second-order accuracy away from discontinuities while simultaneously providing the stability that ensures nonoscillatory solutions. The code has been applied to a number of heliospheric problems, such as the interaction of fast and slow solar wind streams (Odstrcil 1994), distortion of the HCS by shock waves (Odstrcil, Dryer, & Smith 1996), shock-induced magnetic reconnection of coronal sheets (Odstrcil & Karlicky 1997), propagation of CMEs in a structured solar wind (Odstrcil & Pizzo 1999a, 1999b), distortion of the IMF by propagation of CMEs (Odstrcil & Pizzo 1999c), propagation of shock waves in coronal structures (Odstrcil & Karlicky 2000), and global dynamics of magnetic clouds (Vandas & Odstrcil 2000).

The SAIC coronal model, as implemented here, uses a polytropic index of $\gamma = 1.05$ to mimic the near-isothermal nature of the solar corona and thus produce plasma parameters that agree with observed values. On the other hand, the NOAA/SEC code uses $\gamma = 5/3$, in agreement with the observed near adiabatic nature of the solar wind. Ideally, one would like to implement a coronal model incorporating conduction, coronal heating, radiation loss, and Alfvén wave acceleration, together with $\gamma = 5/3$ to provide a seamless boundary between the two models. Unfortunately, practically speaking, such an approach is only now becoming feasible in two dimensions (Lionello, Linker, & Mikić 1999). We have examined the boundary between the two models to estimate what artifacts may have been introduced by allowing γ to vary discontinuously across the boundary. Remarkably, with the exception of temperature (and hence thermal pressure), the magnetofluid parameters remain continuous. The plasma temperature profile with radial distance obviously changes abruptly at the boundary, since $T \propto r^{-2(\gamma-1)}$. Thus, in the coronal model, $T \propto r^{-1/10}$, whereas in the heliospheric model, $T \propto r^{-4/3}$. We are currently exploring improvements to the solar model to remove this artifact. Nevertheless, our analysis suggests that the results will remain qualitatively unaltered.

2.1. *Model Results*

2.1.1. *Configuration of the Ambient Corona and Solar Wind*

The configuration of the solar corona prior to the emergence of the flux rope (but following some energization by photospheric shear) is summarized in Figure 1. Contours of the magnetic flux function (fiduciaries of magnetic field lines in two dimensions) are shown by the solid lines and shaded contours. The flow field is illustrated by the vectors. The system consists of a single streamer belt displaced by $\sim 10^\circ$ below the heliographic equator. Near the Sun, where the flow speeds are smallest, there are significant nonradial flows as the plasma is constrained to flow along magnetic field lines. Farther out ($\sim$2–3 $R_\odot$), as these field lines are dragged by the now fast-flowing solar wind, the flow is essentially radial. In this idealized system, the asymptotic wind speed is the same at all heliographic latitudes. In reality, even the "steady" solar wind is more complex than this. At solar minimum, large polar coronal holes produce uniform high-speed wind at higher latitudes, whereas interaction regions (formed from the interaction of slow and fast streams) at low and midlatitudes are the site of slower and more variable wind. At solar maximum, on the other hand, smaller, mid or equatorial coronal holes produce intermediate, more variable flows within relatively small volumes of the heliosphere, and slow and variable wind occupy the majority of space. The interaction of a flux rope with a more realistic ambient wind requires a three-dimensional treatment and will be the topic of a future study. As an additional simplification, we have neglected the effects of solar rotation. Thus, ambient field lines are radial, and no spiral is generated.

2.1.2. *Eruption of a Flux Rope CME*

Theories of flux rope CMEs generally start from the premise that CMEs are initiated by the release of energy stored in the coronal magnetic field (e.g., Forbes 2000). Previously, we have studied the possibility that eruptions could be initiated by photospheric motions that shear and twist the coronal magnetic field (Mikić, Barnes, & Schnack 1988; Linker & Mikić 1995, 1997; Mikić & Linker 1994). These results show that when the magnetic field is azimuthally

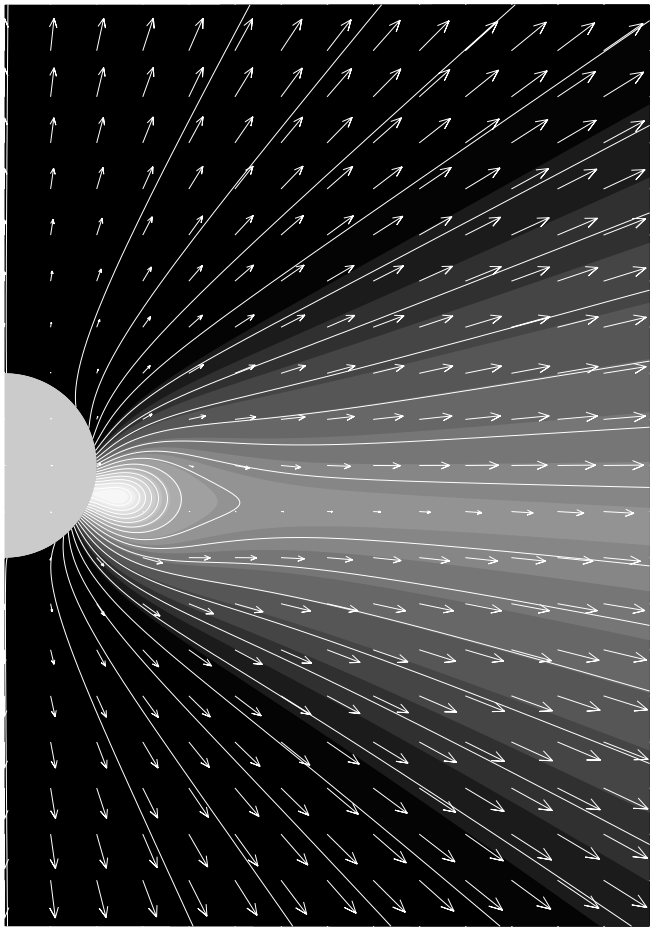

FIG. 1.—Configuration of the solar corona prior to the emergence of the magnetic flux rope. Contours of the magnetic flux function are shown by the solid lines and shaded contours (black to white indicates denotes magnetic flux). The flow field is shown by the arrows.

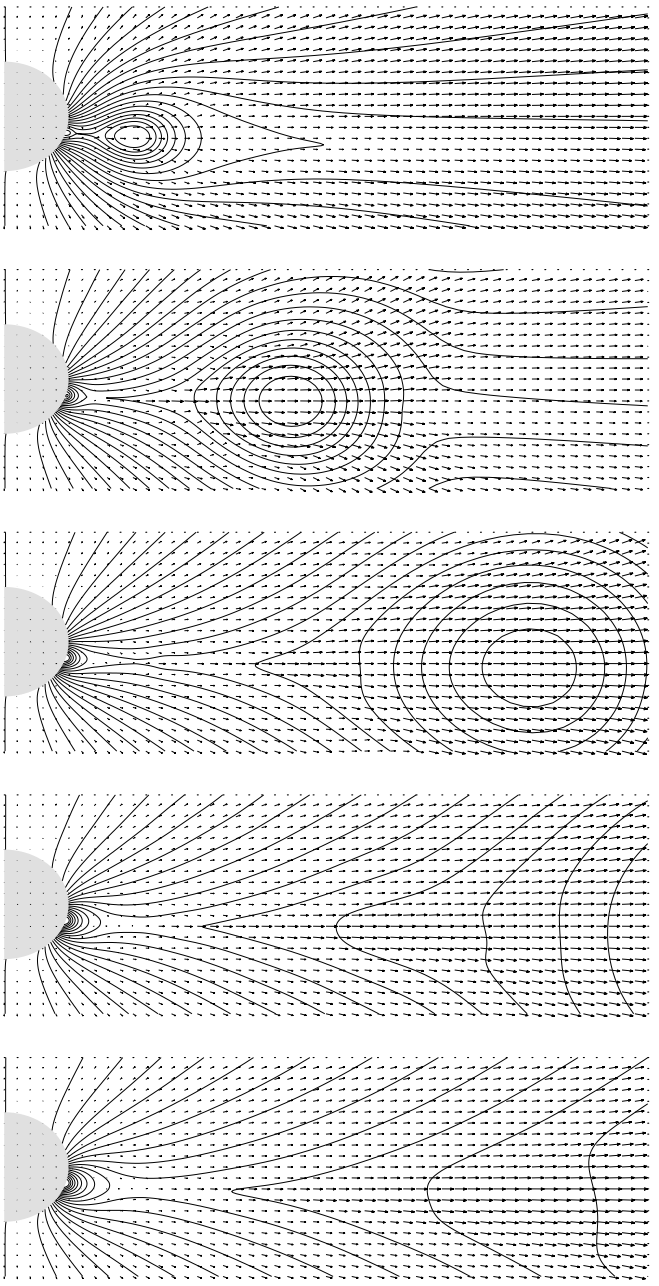

FIG. 2.—Eruption of magnetic flux rope at five sequential times following onset. Magnetic field lines are shown by solid lines, and flow velocities are denoted by the arrows. [*See the electronic edition of the Journal for a color version of this figure.*]

sheared beyond a critical value, helmet streamer configurations can erupt in a manner similar to observed "slow" CMEs, i.e., ejections that are carried out of the corona by the solar wind. It has proved difficult to demonstrate that enough energy can be released rapidly enough by this mechanism to produce a "fast" CME that can drive an interplanetary shock. A more promising mechanism for producing fast CMEs is magnetic flux cancellation. We have found that a reduction in the magnetic flux (i.e., flux cancellation) near the neutral line of a sheared or twisted arcade configuration can lead to the formation of magnetic flux ropes (Amari, Boulmezaoud, & Mikić 1999; Amari et al. 2000; Linker et al. 2001). When the flux cancellation reaches a critical threshold, the entire configuration erupts with the release of a considerable amount of magnetic energy.

In Figure 2 we summarize the launch of just such a flux rope with a sequence of five snapshots following the emergence of new flux. As can be seen, the origins of the flux rope lie in the closed magnetic field lines embedded within the streamer belt. As the flux rope erupts into the solar corona, overlying field lines, which are still connected back to the Sun at both ends, are brought together under the flux rope. As they reconnect with each other, they contribute both to the flux of the evolving flux rope to the antisunward side (*right*) of the reconnection site and to the regrowth of the streamer belt on the sunward side (*left*). Soft X-ray emission observed by the *Yohkoh* spacecraft (Hiei, Hundhausen, & Sime 1993) has been interpreted as the signature of the reformation of the helmet streamer.

In Figure 3 we explore the reconnection site in more detail. The left panel shows magnetic field lines (*solid lines*), flow vectors (*arrows*), and the ϕ component of the current density (J_ϕ) at $\sim$20 hr following the eruption onset. The site of reconnection is clearly visible as the sharp increase in current density near the equatorial plane. The panel on the right shows this region in more detail. The flow pattern is generally directed away from the Sun but develops a significant meridional component near the extended X-type neutral point. In a frame convecting with the ambient solar

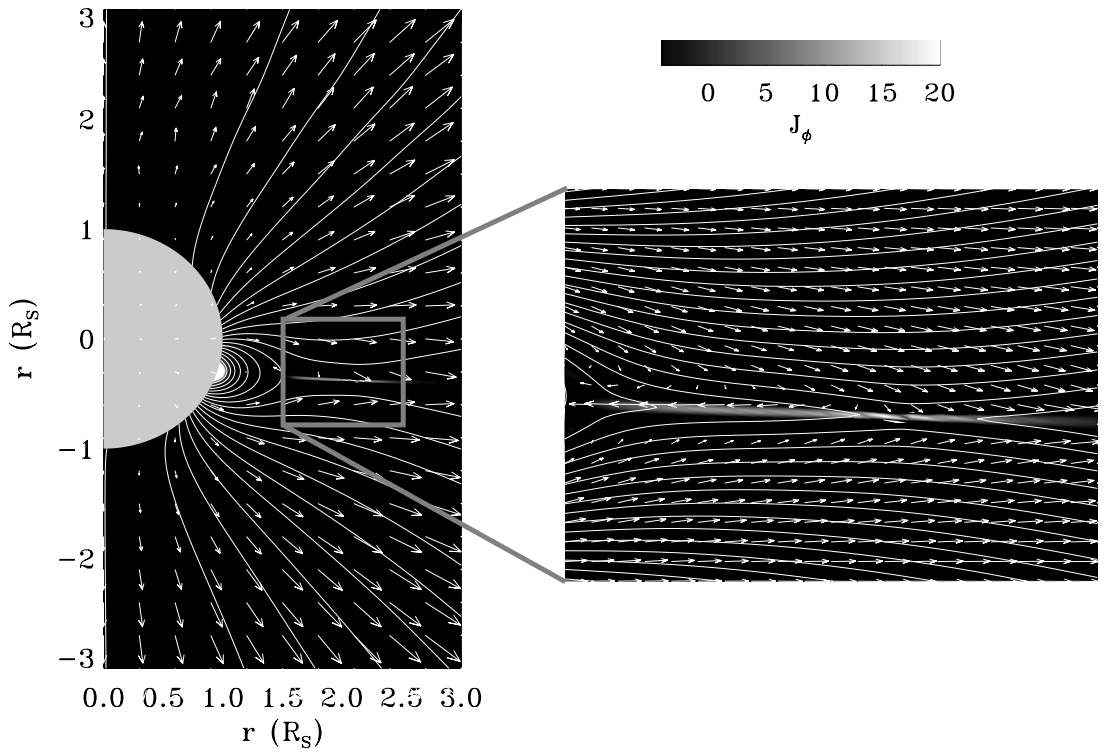

FIG. 3.—Evolution of X-type neutral line underneath the erupting flux rope. Field lines are shown as solid lines, arrows mark the velocity vectors, and the color contours represent the current density in the azimuthal direction (J_ϕ). [*See the electronic edition of the Journal for a color version of this figure.*]

wind, this flow pattern would have the more familiar vertical inflow, such as described by Sweet (1958a, 1958b), Parker (1963), and Petschek (1964). The reconnected outflow does flow away from the X-point in both directions. To the left, it is associated with the rebuilding of the streamer belt, and to the right, it flows away from the Sun, behind the ejected flux rope. Note that in this scenario the plasma populating the new streamer belt came, at least initially, from the reconnected outflow, which in turn had its origins in fast solar wind associated with coronal hole flow.

2.1.3. *Evolution of the CME in the Solar Wind*

In Figure 4 we summarize the evolution of the flux rope and its associated disturbances as it approaches 1 AU ($\sim$215 $R_\odot$). Magnetic field lines within the flux rope are drawn in black, and the colored contours refer to radial velocity. Several features are noteworthy. First, the initially elliptical flux rope first becomes circular then develops into a "pancake" structure as it ploughs into slower ambient solar wind ahead. Second, a fast forward shock, driven by the ejecta, propagates poleward (as a wave) to the boundary of the calculation ($\pm 60^\circ$ heliographic latitude). Third, both the shock and flux rope have developed concave-outward deformations in the vicinity of the plasma sheet as they propagate through the denser medium (Odstrcil et al. 1996). Fourth, the outflow associated with the posteruption reconnection has remained intact within the expansion wave (rarefaction region) behind the flux rope; it has a limited latitudinal extent ($\pm 15^\circ$) and trails the ejecta by $\sim$35 $R_\odot$ (0.16 AU) at 1 AU. Although the peak speed within the ouflow exceeds the speed of the central portion of the flux rope at this time, the large inertia associated with the flux rope ensures that the outflow will never catch up to it. At later times, the speed of the reconnection outflow decays to a fraction of that of the flux rope (see below).

3. IN SITU OBSERVATIONS AND COMPARISON WITH THE MODEL

Given the small angular extent of the reconnection outflow, one might expect to observe such a phenomena only rarely. Moreover, to maintain such a structure out to 1 AU requires a quiescent medium within which to propagate, such as the expansion wave that follows the fast ejecta in our model calculation. We have found several examples of magnetic clouds in the literature that bear striking similarities with the model results, suggesting that indeed such a phenomena is occurring and can be observed. For the purposes of illustration, we study one of the very first observations of a magnetic cloud: the 1968 February 11 event (Klein & Burlaga 1982). The observations are summarized in Figure 5 (*left panels*), where they are compared with the simulation results (*right panels*). Focusing first on the observations, we note that this typical flux rope is moving faster than the ambient solar wind and driving a fast-mode forward shock ahead of it. Within the flux rope, the density and temperature are depressed, while the magnetic field is enhanced. Large coherent rotations can be seen in all three components of the field (not shown). The simulation results show these same basic variations. The lack of an appreciable azimuthal magnetic field in the sheath region (i.e., between the flux rope and the shock wave) can be attributed to the neglect of solar rotation, which would produce azimuthal fields that could then be compressed by the ejecta. Following both the observed and simulated ejecta is a velocity enhancement, lasting $\sim$3/4 day. The observed velocity pulse

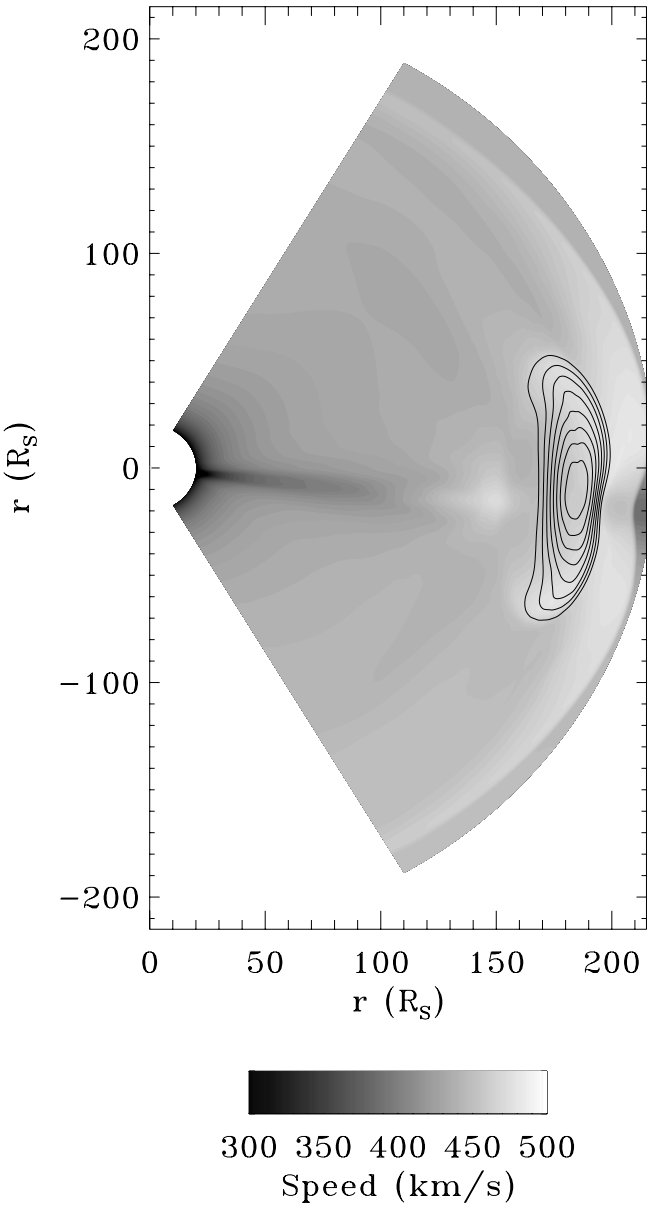

FIG. 4.—Evolution of the flux rope and its associated disturbance as it approaches ~1 AU. Color contours show the speed, and solid lines are contours of the magnetic flux function within the ejecta. [*See the electronic edition of the Journal for a color version of this figure.*]

has an amplitude of ~60 km s^{-1} above ambient solar wind values, while the simulation peaks at ~30 km s^{-1}.

This event has been studied within the approximation of force-free models. Marubashi (1997) computed the latitudinal and longitudinal angles of the axial magnetic field to be $\theta = -10.^{\circ}9$ and $\phi = 238^{\circ}$, respectively, indicating that the flux rope was oriented predominantly in the equatorial plane and obliquely to the radial direction. These values should be viewed with some caution, however, as Lepping, Jones, & Burlaga (1990) found values of $\theta = -29^{\circ}$ and $\phi = 252^{\circ}$ using a similar fitting technique. More relevant to the present study, Marubashi (1997) and Lepping et al. (1990) computed impact parameters (i.e., the distance of closed approach to the axis of the flux rope in units of the flux rope radius) of 0.32 and 0.51, respectively. Thus, the spacecraft apparently did not intercept the flux rope head-on as might have been predicted, given the geometric constraints suggested by the simulation.

4. SUMMARY AND DISCUSSION

The results presented here suggest that velocity enhancements occasionally observed to follow CMEs in the solar wind may be the signatures of posteruptive reconnection underneath the flux rope CME. However, the solar wind displays temporal variability at essentially all times, and we can envisage other processes that could drive a jetlike flow beneath the CME. Thus, these results should be viewed as "discovery" in the sense that while they are new and appealing, more detailed studies are required to substantiate them. A preliminary analysis of 23 magnetic clouds identified in the *Wind* data set (R. P. Lepping 2001, private communication) suggests that 5–10 of these events show evidence of speed enhancements following the cloud. Of these, however, only two events display a smooth, coherent profile, as shown in Figure 5.

The validity of the treatment of magnetic reconnection within the single-fluid MHD approximation is questionable. Although we include a uniform, isotropic resistivity in the coronal model, the limited spatial resolution in the vicinity of the current sheet undoubtedly provides a larger numerical resistivity. We have run cases similar to this at both lower and higher resolution. While the results differ quantitatively, no qualitative differences were found.

Prominence material is occasionally observed in white light at the trailing edges of CMEs near the Sun. Very rarely, density enhancements observed in situ have been associated with prominence material (e.g., Burlaga et al. 1998). Both the reconnection outflow described here and the prominence material might be identified in the plasma data by a density enhancement. The distinguishing characteristic would be the flow velocity profile; if the prominence "lifts" up with the ejecta, no significant velocity enhancement would be predicted. Composition and/or charge state data might show even most dramatic differences; prominence material, being very cold and dense, would be expected to display unusual composition and charge states of the minor ions, while the reconnected outflow described here would show composition characteristics more like ambient solar wind.

It might seem quite remarkable that this signature of reconnection is ever seen considering the turbulent and dynamic nature of the medium into which it is propagating. Fortunately, the fast ejecta acts like an umbrella for the jet signature, sweeping up and deflecting ambient solar wind ahead and creating an expansion wave behind it, into which the jet signature can propagate and maintain its coherence.

The simulation suggests that the reconnection process occurs on a spatial scale much smaller than the scale size of the flux rope. Thus, to observe such signatures, spacecraft trajectories must intercept flux ropes near their axis. This was not the case for the 1969 February 11 event, where analysis indicates that the spacecraft intercepted the cloud between 30% and 50% away from its axis. Several interpretations are possible: (1) the observed velocity enhancement was not the result of posteruptive reconnection outflow, (2) the reconnection site was displaced in latitude from the axis of the flux rope (i.e., the eruption geometry was asymmetric), or (3) the latitudinal extent of the reconnected outflow is larger than that suggested by

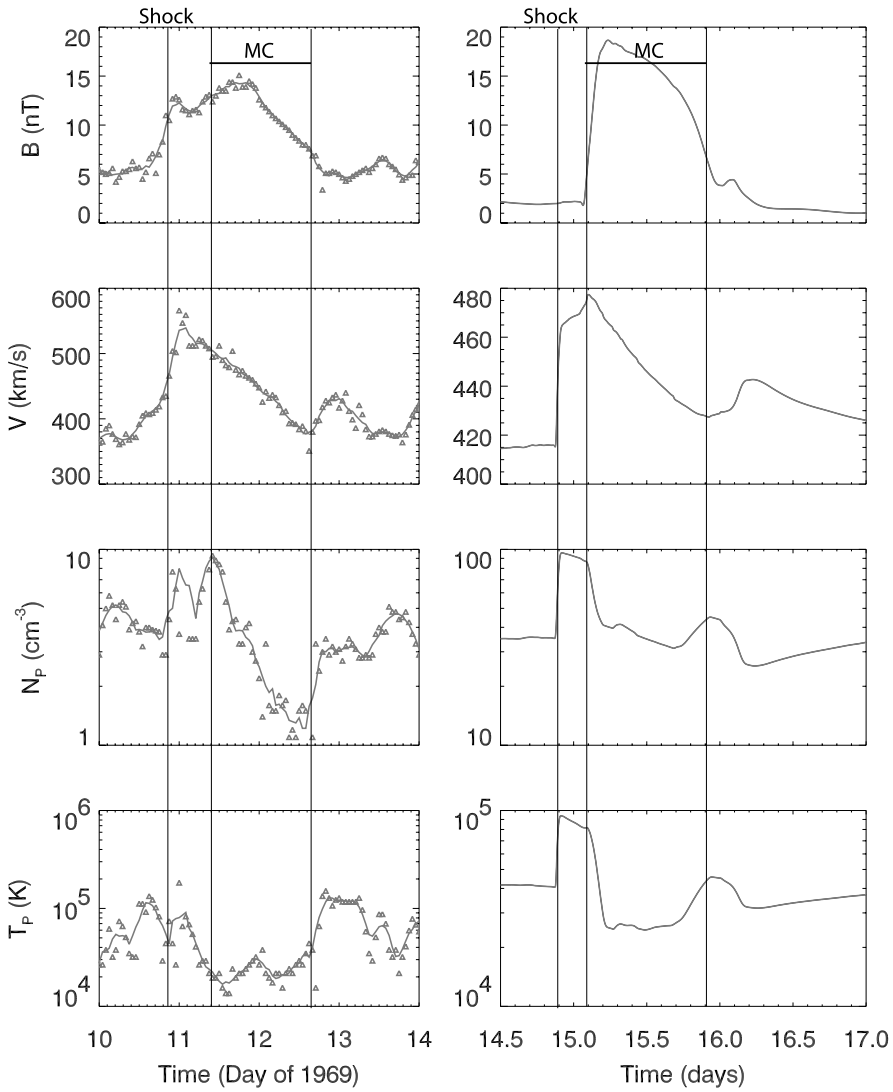

FIG. 5.—*Left*: Comparison of in situ measurements of (B) magnetic field strength, (V) flow speed, (N_p) proton number density, and (T_p) proton temperature with simulation results (*right*). Vertical lines mark the inferred location of the magnetic cloud (*flux rope*) and the shock preceding it. For the left panels, the triangles show 1 hr averaged data, whereas the solid line has been boxcar-averaged over five points. For the right panels, the time is measured since the onset of the eruption. [*See the electronic edition of the Journal for a color version of this figure.*]

the simulation. Given that one of the latter two scenarios is the correct interpretation, we could in principle use the information to constrain models of CME initiation and eruption.

Should these results be further substantiated, they may allow us to distinguish between competing theories of CME models. In particular, the "breakout" model (Antiochos 1998), which predicts reconnection to occur above the flux rope and not below it, would not be reconcilable with these observations. Of course, given that most CMEs do not apparently exhibit such velocity enhancements, we hasten to add that this does not invalidate the applicability of this mechanism to the vast majority of flux-rope CMEs.

In closing, we reiterate that while these results require further substantiation, our simulations suggest that post-'eruptive reconnection, occurring underneath a flux-rope CME, occurs and may remain intact out to 1 AU and beyond.

The authors gratefully acknowledge the support of the National Aeronautics and Space Administration (Sun-Earth Connections Theory Program, Supporting Research and Technology Programs, and *SOHO* Guest Investigator Program) and the National Science Foundation (STC ATM 9613834) in undertaking this study. D. F. W. acknowledges the support of the National Aeronautics and Space Administration (Living with a Star Program, NAG 5-10833). We also thank the San Diego Supercomputer Center and the National Center for Atmospheric Research (both supported by the National Science Foundation) and the National Energy Research Supercomputer Center for providing computational support.

REFERENCES

Amari, T., Boulmezaoud, T., & Mikić, Z. 1999, A&A, 350, 1051
Amari, T., Lucini, J. F., Mikić, Z., & Linker, J. A. 2000, ApJ, 529, L49
Antiochos, S. K.1998, ApJ, 502, L181
Burlaga, L. F. 1988, J. Geophys. Res., 93, 7217
Collier, M. R., et al. 2001, J. Geophys. Res., 106, 15985
Forbes, T. G. 2000, J. Geophys. Res., 105, 23153
Gosling, J. T., Birn, J., & Hesse, M. 1995, Geophys. Res. Lett., 22, 869
Hiei, E., Hundhausen, A. J., & Sime, D. G. 1993, Geophys. Res. Lett., 20, 2785
Hundhausen, A. J. 1988, in Proc. 6th. International Solar Wind Conf., ed. V. J. Pizzo, T. E. Holzer, & D. G. Sime (Boulder: NCAR), 181
Klein, L. W., & Burlaga, L. F. 1982, J. Geophys. Res., 87, 613
Klimchuk, J. A. 2001, in Space Weather (Geophys. Monogr. 125; Washington, DC: AGU), 143
Lepping, R. P., Jones, J. A., & Burlaga, L. F. 1990, J. Geophys. Res., 95, 11957
Linker, J. A., & Mikić, Z. 1996, in AIP Conf. Proc. 382, Solar Wind 8, ed. D. Winterhalter, J. T. Gosling, S. R. Habbal, W. S. Kurth, & M. Neugebauer (New York: AIP), 60
———. 1997, AAS, SPD, 28, 06.01
Linker, J. A., Mikić, Z., Lionello, R., & Riley, P. 2001, in Proc. AGU Spring Meeting (: AGU), SH31, C04L
Lionello, R., Linker, J. A., & Mikić, Z. 1999, J. Comput. Phys., 152, 346
Lionello, R., Velli, M., Einaudi, G., & Mikić, Z. 1998, ApJ, 494, 840
Marubashi, K. 1997, Coronal Mass Ejections (Geophys. Monogr. 99; Washington, DC: AGU), 147
Mikić, Z., Barnes, D. C., & Schnack, D. D. 1988, ApJ, 328, 830
Mikić, Z., & Linker, J. A. 1994, ApJ, 430, 898
Mikić, Z., Linker, J. A., Schnack, D. D., Lionello, R., & Tarditi, A. 1999, Phys. Plasmas, 6, 2217
Odstrcil, D. 1993, J. Comput. Phys., 108, 218
———. 1994, J. Geophys. Res., 99, 17,653
Odstrcil, D., Dryer, M., & Smith, Z. 1996, J. Geophys. Res., 101, 19,973
Odstrcil, D., & Karlicky, M. 1997, Adv. Space Res., 19, 1895
———. 2000, A&A, 359, 766
Odstrcil, D., Linker, J. A., Lionello, R., Mikic, Z., Riley, P., Pizzo, V. J., & Luhmann, J. 2002, J. Geophys. Res., submitted
Odstrcil, D., & Pizzo, V. J. 1999a, J. Geophys. Res., 104, 483
———. 1999b, J. Geophys. Res., 104, 493
———. 1999c, J. Geophys. Res., 104, 28,225
Parker, E. N. 1963, Interplanetary Dynamical Processes (New York: Interscience)
Petschek, H. E. 1964, in Proc. AAS-NASA Symp., The Physics of Solar Flares, ed. W. N. Hess (NASA SP-50; Washington, DC: NASA), 425
Riley, P., Linker, J. A., Mikic, Z., Zurbuchen, T. H., Lario, D., & Lepping, R. P. 2002, J. Geophys. Res., submitted
Sonnerup, B. U. O. 1970, J. Plasma Phys., 4, 161
Sweet, P. A. 1958a, Nuovo Cimento Suppl., 8, 188
———. 1958b, IAU Symp., 6, Electromagnetic Phenomena in Cosmical Physics, ed. B. Lehnert (Cambridge: Cambridge Univ. Press), 123
Toth, G., & Odstrcil, D. 1996, J. Comput. Phys., 128, 82
Vandas, M., & Odstrcil, D. 2000, J. Geophys. Res., 105, 12,605